9486 *Inorg. Chem.* **2010**, *49*, 9486–9496
DOI: 10.1021/ic101211n

Inorganic Chemistry
Article

# Ag(I) Organometallic Coordination Polymers and Capsule with Tris-Allyl Cyclotriveratrylene Derivatives

**Marc A. Little,[†] Malcolm A. Halcrow,[†] Lindsay P. Harding,[‡] and Michaele J. Hardie*,[†]**

[†]*School of Chemistry, University of Leeds, Leeds, LS2 9JT, U.K., and* [‡]*Department of Chemical and Biological Sciences, University of Huddersfield, Huddersfield, HD1 3DH, U.K.*

Received June 17, 2010

Tris-allyl-cyclotriguaiacylene combines with silver salts to give a range of crystalline network structures and one discrete complex. A number of different coordination modes are found within the complexes including $\eta^2$-allyl, aryl, and OR groups binding to Ag(I). $AgSbF_6$ gives two types of three-dimensional (3-D) coordination polymer with unusual topologies, along with a discrete $Ag_2L_2$ capsule dependent on reaction stoichiometry and reaction conditions. Isostructural coordination chain structures are found with $AgBF_4$ and $AgClO_4$, while use of $Ag(CF_3SO_3)$ gives two-dimensional (2-D) and 3-D coordination polymers through bridging triflate anions.

## Introduction

The study of polymeric metal−ligand assemblies, termed metal−organic frameworks or coordination polymers, has burgeoned recently with the realization that by using bridging functionality and stereochemistry as design principles complexes with regular two-dimensional (2-D) and three-dimensional (3-D) network structures can be assembled.[1,2] Potential applications for coordination polymers are far-reaching and have been demonstrated or mooted in the fields of magnetism, non-linear optics, catalysis, separations and extractions, gas storage, and other zeolitic applications.[1]

A large number of coordination polymers involving Ag(I) are known.[2] Because of its lack of crystal field effects Ag(I) may adopt a variety of stereochemistries, and coordination polymers with Ag(I) are therefore structurally diverse and often show marked structural variations with different anions. While the majority of Ag(I) coordination polymers involve coordination interactions from hetereoatoms, Ag(I) coordination polymers featuring organometallic interactions to the metal have also been reported.[3−5] In many cases these organometallic polymers also include additional coordination interactions from heteroatoms with the organic ligands or counter-anions. Ag(I) organometallic coordination polymers with host-type ligands are not well-known, although examples with calixarene and crown ether are known.[4] Steel and co-workers have recently reported systematic studies with different isomers of divinylbenzene utilizing the silver-alkene interaction as a supramolecular synthon.[5] They observed both discrete and polymeric complexes, and the most commonly observed organometallic ligand binding mode was an $\eta^2$ interaction from the vinyl units.

We have recently reported a number of coordination polymers with tripodal ligands related to the cyclotriveratrylene (CTV) molecular host,[6,7] and Holman has reported a coordination polymer based on cryptophanes which are covalently linked bis-CTVs.[8] CTV is a relatively rigid

*To whom correspondence should be addressed. E-mail: m.j.hardie@leeds.ac.uk.

(1) For examples of reviews see: (a) Perry, J. J.; Perman, J. A.; Zaworotko, M. J. *Chem. Soc. Rev.* **2009**, *48*, 3018. (b) Noro, S.; Kitagawa, S.; Akutagawa, T.; Nakamura, T. *Prog. Polym. Sci.* **2009**, *34*, 240. (c) Robin, A. Y.; Fromm, K. M. *Coord. Chem. Rev.* **2006**, *250*, 2127. (d) Ockwig, N. W.; Delgado-Friedrichs, O.; O'Keeffe, M.; Yaghi, O. M. *Acc. Chem. Res.* **2005**, *38*, 176. (e) Janiak, C. *Dalton Trans.* **2003**, 2781. (f) James, S. L. *Chem. Soc. Rev.* **2003**, *32*, 276. (g) Robson, R. *Dalton Trans.* **2000**, 3735.

(2) For reviews see: (a) Steel, P. J.; Fitchett, C. M. *Coord. Chem. Rev.* **2008**, *252*, 990. (b) Chen, C.-L.; Kang, B.-S.; Su, C.-Y. *Aust. J. Chem.* **2006**, *59*, 3. (c) Khlobystov, A. N.; Blake, A. J.; Chapmness, N. R.; Lemenovskii, D. A.; Majouga, A. G.; Zyk, N. V.; Schröder, M. *Coord. Chem. Rev.* **2001**, *222*, 155.

(3) For example: (a) Bashiri, R.; Akhbari, K.; Morsali, A.; Zeller, M. *J. Organomet. Chem.* **2008**, *693*, 1903. (b) Mak, T. C. W.; Zhao, L. *Chem. Asian J.* **2007**, *2*, 456. (c) Dong, Y.-B.; Geng, Y.; Ma, J.-P.; Huang, R.-Q. *Organometallics* **2006**, *25*, 447. (d) Cottam, J. R. A.; Steel, P. J. *J. Organomet. Chem.* **2006**, *691*, 2286. (e) Lim, K. C.; Marchetti, F.; Pettinari, C.; Skelton, B. W.; Smith, B. W.; White, A. H. *Inorg. Chim. Acta* **2006**, *359*, 1594. (f) Wang, P.; Dong, Y.-B.; Ma, J.-P.; Huang, R.-Q.; Smith, M. A. *Cryst. Growth Des.* **2005**, *5*, 701. (g) Dong, Y.-B.; Zhang, Q.; Wang, L.; Ma, J.-P.; Huang, R.-Q.; Shen, D.-Z.; Chen, D.-Z. *Inorg. Chem.* **2005**, *19*, 6591. (h) Liu, S. Q.; Kuroda-Sowa, T.; Konaka, H.; Suenaga, Y.; Maekawa, M.; Mizutani, T.; Ning, G. L.; Munakata, M. *Inorg. Chem.* **2005**, *44*, 1031. (i) Wen, M.; Munakata, M.; Suenaga, Y.; Kuroda-Sowa, T.; Maekawa, M. *Inorg. Chim. Acta* **2002**, *340*, 8. (j) Steel, P. J.; Webb, N. C. *Eur. J. Inorg. Chem.* **2002**, 2257. (k) Munakata, M.; Wu, L. P.; Ning, G. L.; Kuroda-Sowa, T.; Maekawa, M.; Suenaga, Y.; Maeno, N. *J. Am. Chem. Soc.* **1999**, *121*, 4968.

(4) (a) Budka, J.; Lhotak, P.; Stibor, I.; Sykora, J.; Cisarova, I. *Supramol. Chem.* **2003**, *15*, 353. (b) Prince, P. D.; Cragg, P. J.; Steed, J. W. *Chem. Commun.* **1999**, 1179.

(5) Burgess, J.; Cottam, J. R. A.; Steel, P. J. *Aust. J. Chem.* **2006**, *59*, 295.

(6) (a) Sumby, C. J.; Hardie, M. J. *Cryst. Growth Des.* **2005**, *5*, 1321. (b) Hardie, M. J.; Sumby, C. J. *Inorg. Chem.* **2004**, *43*, 6872. (c) Ronson, T. K.; Hardie, M. J. *CrystEngComm* **2008**, *10*, 1731.

(7) Sumby, C. J.; Fisher, J.; Prior, T. J.; Hardie, M. J. *Chem.—Eur. J.* **2006**, *12*, 2945.

(8) Mough, S. T.; Holman, K. T. *Chem. Commun.* **2008**, 1407.


Published on Web 09/23/2010

molecular host,[9] and CTV and its analogues have found applications in a variety of areas including, but not restricted to, soft materials such as gels[10] and liquid crystals,[11] sensors for molecular and ionic guests,[12] in biomimetic studies,[13] molecular separations,[14] and within large discrete organic[15,16] and metallo-supramolecular systems.[17] Tripodal analogues of CTV are often accessed via chiral cyclotriguaiacylene (CTG), and the synthetic route to CTG proceeds via the tris-allyl derived ligand **1**.[18] Following Steel and co-workers studies on divinylbenzene and Ag(I), we investigated the possibility of forming organometallic supramolecular assemblies with ligand **1** and Ag(I), noting ligand **1** has three available vinyl units attached to a rigid pyramidal framework.

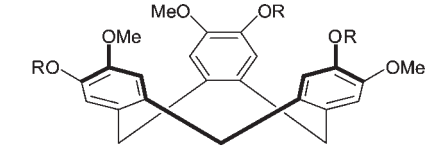


R = $CH_3$ **CTV**
= H **CTG**

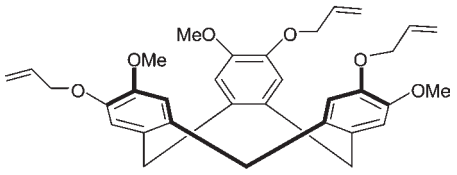


**1**

Previously reported Ag(I) complexes of CTV, or of related hosts, are coordination complexes, with binding of Ag(I) through additional N-donor moieties[6,7] or through the methoxy groups of CTV in discrete and polymeric complexes.[19,20] One previous reported example of an organometallic interaction occurs in the complex $[Ag(CH_3CN)(H_2O)(CTV)_2]^+$ where a capsule-like assembly was formed in the solid state with Ag(I) binding to one CTV through two long $\eta^1$ interactions to different arene rings.[19] Reported herein are the coordination polymers formed from the reaction of **1** with a variety of silver salts. In general, a range of polymer types were observed from one-dimensional (1-D) chains to highly complicated 3-D networks. The binding mode of ligand **1** to the Ag(I) varies considerably from complex to complex.

## Experimental Section

Ligand **1** was synthesized as a racemic mixture by literature methods.[18] Reagents were obtained from commercial sources and used as received. Elemental analyses were obtained on a Carlo Erba Elemental Analyzer MOD 1106 instrument and performed by the service of the School of Chemistry at the University of Leeds. The Electrospray (ES) mass spectrum was recorded using a Bruker MicroToF-q mass spectrometer. $^1$H Nuclear Magnetic Resonance spectra were recorded using a Bruker Avance 500 instrument. Infrared spectra were recorded on a Perkin-Elmer FTIR spectrometer and samples analyzed as solids.

**Synthesis. Complex $[Ag_9(\mathbf{1})_7(H_2O)_3]\cdot(\mathbf{1})\cdot 9(SbF_6)\cdot n$(solvent) 2.** Plate-like crystals of the complex were obtained on slow diffusion of diethylether into a solution of **1** (10.0 mg, 0.0189 mmol) and $Ag(SbF_6)$ (14.3 mg, 0.0566 mmol) in $MeNO_2$ (0.60 mL). The crystals were collected by filtration, washed with diethylether and dried in air. Yield 13.6 mg: 77%.

IR Spectra (solid state, $\nu$ cm$^{-1}$): 3300−3650 (s), 2850−3050 (s), 2610 (w), 1608 (m), 1557 (m), 1506 (s), 1469 (m), 1446 (m), 1425 (m), 1398 (m), 1345 (m), 1261 (s), 1217 (m), 1194 (m), 1143 (m), 1084 (m), 1018 (m), 971 (m), 943 (m), 885 (w), 858 (m), 788 (w), 748 (m), 711 (w), 657 (s), 622 (m), 579 (w), 547 (w). Elemental analysis for $C_{264}H_{294}Ag_9F_{54}O_{51}Sb_9.2MeNO_2.3Et_2O$ after crystals were dried in vacuo, found, (calcd) (%): C 43.35 (43.25), H 4.15 (4.31), N 0.45 (0.36). $^1$H NMR ($CD_3NO_2$, 500 MHz): $\delta$ (ppm.) 3.46 (d, 3H, $^2J_{HH}$ = 13.90 Hz, $CH_2$), 3.87 (s, 9H, OMe), 4.53 (broad d, 6H, O−$CH_2$), 4.68 (dd, 3H, $^2J_{HH}$ = 12.75 Hz, $^3J_{HH}$ = 5.14 Hz, $CH_2$), 5.43 (d, 3H, $^3J_{HH}$ = 10.15 Hz (cis), CH=C$\underline{H}_2$), 5.53 (d, 3H, $^3J_{HH}$ = 17.05 Hz (trans), CH=C$\underline{H}_2$), 6.40 (m, 3H, C$\underline{H}$=$CH_2$), 7.06 (s, 6H, 2 × CH aryl).

**Complex $[Ag_2(\mathbf{1})_2]\cdot 2(SbF_6)\cdot n$(solvent) 3.** Long thin needle crystals of the complex were obtained on slow diffusion of diisopropylether into a solution of **1** (5.0 mg, 0.0095 mmol) and $Ag(SbF_6)$ (3.3 mg, 0.0096 mmol) in $MeNO_2$ (0.30 mL). The crystals were collected by filtration, washed with diisopropylether, and dried in air. Yield 5.1 mg: 61%.

IR Spectra (solid state, $\nu$ cm$^{-1}$): 2800−3100 (s), 1645 (w), 1607 (m), 1510 (s), 1458 (m), 1423 (m), 1397 (m), 1344 (m), 1258 (s), 1217 (s), 1192 (s), 1148 (s), 1086 (s), 1019 (m), 924 (s), 885 (m), 847 (m), 738 (m), 661 (m), 617 (s), 584 (w), 537 (w). Elemental analysis for $C_{66}H_{72}Ag_2F_{12}O_{12}Sb_2.2H_2O.0.5(MeNO_2)$ after crystals were dried in vacuo, found, (calcd) (%): C 43.80, (44.08), H 3.95 (4.31), N 0.35 (0.39). $^1$H NMR ($CD_3NO_2$, 500 MHz): $\delta$ (ppm.) 3.54 (d, 3H, $^2J_{HH}$ = 13.62 Hz, $CH_2$), 3.84 (s, 9H, OMe), 4.59 (m, 6H, O−$CH_2$), 4.71 (d, 3H, $^2J_{HH}$ = 13.72 Hz, $CH_2$), 5.30 (d, 3H, $^3J_{HH}$ = 10.25 Hz (cis), CH=C$\underline{H}_2$), 5.43 (d, 3H, $^3J_{HH}$ = 17.08 Hz (trans), CH=C$\underline{H}_2$), 6.22 (m, 3H, C$\underline{H}$=$CH_2$), 7.03 (s, 3H, CH aryl), 7.05 (s, 3H, CH aryl).

**Complex $[Ag_2(\mathbf{1})_2]\cdot 2(SbF_6)\cdot 4(MeNO_2)$ 4.** Hexagonal crystals of the complex were obtained on slow diffusion of diisopropylether into a solution of **1** (5.0 mg, 0.0095 mmol) and $Ag(SbF_6)$ (1.6 mg, 0.0048 mmol) in $MeNO_2$ (0.7 mL). The crystals were collected by filtration, washed with diisopropylether and dried in air. Yield 2.8 mg: 67%.

IR Spectra (solid state, $\nu$ cm$^{-1}$): 3400−3600 (w), 2800−3000 (m), 1608 (m), 1556 (s), 1508 (s), 1463 (s), 1401 (s), 1401 (s), 1378 (m), 1344 (m), 1258 (s), 1219 (m), 1195 (m), 1145 (s), 1086 (s),

(9) For examples of reviews see: (a) Brotin, T.; Dutasta, J.-P. *Chem. Rev.* **2009**, *109*, 88. (b) Hardie, M. *Chem. Soc. Rev.* **2010**, *39*, 516. (c) Collet, A. *Tetrahedron* **1987**, *43*, 5725.

(10) (a) Westcott, A.; Sumby, C. J.; Walshaw, R. D.; Hardie, M. J. *New J. Chem.* **2009**, *33*, 902. (b) Bardelang, D.; Camerel, F.; Ziessel, R.; Schmutz, M.; Hannon, M. J. *J. Mater. Chem.* **2008**, *18*, 489. (c) Kubo, Y.; Yoshizumi, W.; Minami, T. *Chem. Lett.* **2008**, *37*, 1238.

(11) (a) Rio, Y.; Nierengarten, J.-F. *Tetrahedron Lett.* **2002**, *43*, 4321. (b) Felder, D.; Heinrich, B.; Guillon, D.; Nicoud, J.-F.; Nierengarten, J.-F. *Chem.—Eur. J.* **2000**, *6*, 3501.

(12) (a) Dumartin, M.-L.; Givelet, C.; Meyrand, P.; Bibal, B.; Gosse, I. *Org. Biomol. Chem.* **2009**, *7*, 2725. (b) Moriuchi-Kawakami, T.; Sato, J.; Shibutani, Y. *Anal. Sci.* **2009**, *25*, 449. (c) Zhang, S.; Echegoyen, L. *J. Am. Chem. Soc.* **2005**, *127*, 2006. (d) Gawenis, J. A.; Holman, T. K.; Atwood, J. L.; Jurisson, S. S. *Inorg. Chem.* **2002**, *41*, 6028.

(13) Maiti, D.; Woertink, J. S.; Ghiladi, R. A.; Solomon, E. I.; Karlin, K. D. *Inorg. Chem.* **2009**, *48*, 8342.

(14) Huerta, E.; Cequier, E.; de Mendoza, J. *Chem. Commun.* **2007**, 5016.

(15) Percec, V.; Imam, M. R.; Peterca, M.; Wilson, D. A.; Heiney, P. A. *J. Am. Chem. Soc.* **2009**, *131*, 1294.

(16) (a) Xu, D.; Warmuth, R. *J. Am. Chem. Soc.* **2008**, *130*, 7520. (b) Strübe, J.; Neumann, B.; Stammler, H.-G.; Kuck, D. *Chem.—Eur. J.* **2009**, *15*, 2256.

(17) For example: (a) Ronson, T. K.; Fisher, J.; Harding, L. P.; Rizkallah, P. J.; Warren, J. E.; Hardie, M. J. *Nat. Chem.* **2009**, *1*, 212. (b) Ronson, T. K.; Fisher, J.; Harding, L. P.; Hardie, M. J. *Angew. Chem., Int. Ed.* **2007**, *46*, 9086. (c) Zhong, Z.; Ikeda, A.; Shinkai, S.; Sakamoto, S.; Yamaguchi, K. *Org. Lett.* **2001**, *3*, 1085.

(18) For example: Canceill, J.; Collet, A.; Gottarelli, G. *J. Am. Chem. Soc.* **1984**, *106*, 5997.

(19) Ahmad, R.; Hardie, M. J. *Cryst. Growth Des.* **2003**, *3*, 493.

(20) Ahmad, R.; Hardie, M. J. *CrystEngComm* **2002**, *4*, 227.

1023 (m), 886 (m), 860 (s), 789 (w), 749 (m), 715 (w), 654 (s), 622 (m), 577 (w), 545 (w). Elemental analysis for $C_{66}H_{72}Ag_2F_{12}O_{12}Sb_2 \cdot 4MeNO_2$ after crystals were dried in vacuo, found, (calcd) (%): C 42.50, (42.26), H 4.55 (4.26), N 2.44 (2.82). $^1$H NMR ($CD_3NO_2$, 500 MHz): $\delta$ (ppm.) 3.55 (d, 3H, $^2J_{HH}$ = 13.76 Hz, $CH_2$), 3.83 (s, 9H, OMe), 4.59 (m, 6H, O−$CH_2$), 4.73 (d, 3H, $^2J_{HH}$ = 13.72 Hz, $CH_2$), 5.29 (d, 3H, $^3J_{HH}$ = 11.33 Hz (cis), CH=C$H_2$), 5.42 (d, 3H, $^3J_{HH}$ = 17.08 Hz (trans), CH=C$H_2$), 6.19 (m, 3H, C$H$=$CH_2$), 7.03 (s, 3H, CH aryl), 7.05 (s, 3H, C$H$-aryl). ES MS ($MeNO_2$ solution): $m/z$ 2037.5 $\{[Ag_2(\mathbf{1})_3](SbF_6)\}^+$ (calcd 2036.3); 1693.7 $[Ag(\mathbf{1})_3]^+$ (calcd 1692.6); 1507.2 $\{[Ag_2(\mathbf{1})_2](SbF_6)\}^+$ (calcd 1508.0); 1165.4 $[Ag(\mathbf{1})_2]^+$ (calcd 1164.4); 635.4 $[Ag(\mathbf{1})]^+$ (calcd 636.1).

**$[Ag_2(\mathbf{1})(H_2O)_2]\cdot 2(BF_4)\cdot 2(MeNO_2)$ 5.** Small needle crystals of the complex were obtained on slow diffusion of diethylether into a solution of **1** (10.0 mg, 0.0189 mmol) and $[Ag(MeCN)_4](BF_4)$ (20.4 mg, 0.0566 mmol) in $MeNO_2$ (0.60 mL). The crystals were collected by filtration, washed with diethylether and dried in air. Yield 12.5 mg: 72%.

IR Spectra (solid state, $\nu$ cm$^{-1}$): 3400−3550 (s), 2850−3000 (w), 1607 (w), 1548 (w), 1509 (s), 1479 (m), 1467 (m), 1426 (w), 1400 (m), 1344 (w), 1263 (s), 1217 (m), 1196 (m), 1146 (m), 950−1100 (s), 927 (w), 888 (w), 863 (w), 749 (w), 741 (w), 657 (w), 619 (m), 544 (w). Elemental analysis for $C_{33}H_{40}Ag_2B_2F_8O_8 \cdot MeNO_2$ after crystals were dried in vacuo, found, (calcd) (%): C 39.95, (40.20), H 4.10 (4.27), N 1.35 (1.38). $^1$H NMR ($CD_3NO_2$, 500 MHz): $\delta$ (ppm.) 3.59 (d, 3H, $^2J_{HH}$ = 13.12 Hz, $CH_2$), 3.83 (s, 9H, OMe), 4.60 (m, 6H, O−$CH_2$), 4.79 (d, 3H, $^2J_{HH}$ = 13.28 Hz, $CH_2$), 5.28 (d, 3H, $^3J_{HH}$ = 8.98 Hz (cis), CH=C$H_2$), 5.40 (d, 3H, $^3J_{HH}$ = 15.63 Hz (trans), CH=C$H_2$), 6.16 (m, 3H, C$H$=$CH_2$), 7.03 (s, 3H, CH aryl), 7.05 (s, 3H, C$H$-aryl).

**Complex $[Ag_2(\mathbf{1})(H_2O)_2]\cdot 2(ClO_4)\cdot 2(MeNO_2)$ 6.** Long thin needle crystals of the complex were obtained on slow diffusion of diethylether into a solution of **1** (10.0 mg, 0.0189 mmol) and $AgClO_4 \cdot H_2O$ (12.8 mg, 0.0566 mmol) in $MeNO_2$ (0.60 mL). The crystals were collected by filtration, washed with diethylether, and dried in air. Yield 14.2 mg: 68%.

IR Spectra (solid state, $\nu$ cm$^{-1}$): 3200−3500 (m), 2900−3000 (w), 2016 (w), 1608 (s), 1508 (s), 1479 (s), 1465 (s), 1425 (m), 1400 (m), 1344 (m), 1260 (s), 1217 (m), 1196 (m), 980−1150 (s), 977 (s), 927 (m), 888 (m), 861 (m), 749 (m), 715 (w), 656 (w), 621 (s), 546 (w). Elemental analysis for $C_{33}H_{40}Ag_2Cl_2O_{16} \cdot H_2O$ after crystals were dried in vacuo, found, (calcd) (%): C 41.25, (41.23); H 4.00, (3.98). $^1$H NMR ($CD_3NO_2$, 500 MHz): $\delta$ (ppm.) 3.49 (d, 3H, $^2J_{HH}$ = 13.86 Hz, $CH_2$), 3.90 (s, 9H, OMe), 4.56 (broad d, 6H, $^3J_{HH}$ = 15.07 Hz, O−$CH_2$), 4.73 (dd, 3H, $^2J_{HH}$ = 13.75 Hz, $^3J_{HH}$ = 4.94 Hz, $CH_2$), 5.52 (d, 3H, $^3J_{HH}$ = 10.15 Hz (cis), CH=C$H_2$), 5.61 (d, 3H, $^3J_{HH}$ = 17.16 Hz (trans), CH=C$H_2$), 6.54 (m, 3H, C$H$=$CH_2$), 7.09 (s, 6H, 2 x CH aryl).

**Complex $[Ag_2(\mathbf{1})(OTf)_2]$ 7.** Small needle crystals of the complex were obtained on slow diffusion of diethylether into a solution of **1** (10.0 mg, 0.0189 mmol) and Ag(OTf) (14.6 mg, 0.0566 mmol) in $MeNO_2$ (0.60 mL). The crystals were collected by filtration, washed with diethylether, and dried in air. Yield 17.7 mg: 90%.

IR Spectra (solid state, $\nu$ cm$^{-1}$): 2800−3000 (m), 1607 (m), 1505 (s), 1456 (m), 1401 (m), 1341 (m), 1248 (s), 1217 (s), 1190 (s), 1158 (s), 1106 (m), 1074 (s), 1021 (s), 955 (m), 916 (m), 892 (m), 874 (m), 759 (w), 741 (m), 620 (s), 575 (m), 521 (m). Elemental analysis for $C_{35}H_{36}Ag_2F_6O_{12}S_2$ after crystals were dried in vacuo, found, (calcd) (%): C 40.25, (40.31); H 3.60, (3.48). $^1$H NMR ($CD_3NO_2$, 500 MHz): $\delta$ (ppm.) 3.53 (d, 3H, $^2J_{HH}$ = 12.92 Hz, $CH_2$), 3.88 (s, 9H, OMe), 4.50−4.75 (m, 9H, O−$CH_2$, $CH_2$), 5.48 (d, 3H, $^3J_{HH}$ = 9.88 Hz (cis), CH=C$H_2$), 5.59 (d, 3H, $^3J_{HH}$ = 17.58 Hz (trans), CH=C$H_2$), 6.49 (m, 3H, C$H$=$CH_2$), 7.09 (s, 3H, CH aryl), 7.10 (s, 3H, C$H$-aryl).

**Complex [Ag(1)(OTf)] 8.** Small needle crystals of the complex were obtained on slow diffusion of diisopropylether into a solution of **1** (5.0 mg, 0.0095 mmol) and Ag(OTf) (1.2 mg, 0.0048 mmol) in $MeNO_2$ (0.4 mL). The crystals were collected by filtration, washed with diisopropylether, and dried in air. Yield 2.8 mg: 73%.

IR Spectra (solid state, $\nu$ cm$^{-1}$): 3300−3500 (w), 2850−3050 (m), 1604 (m), 1587 (m), 1505 (s), 1475 (m), 1459 (m), 1428 (w), 1410 (m), 1397 (m), 1389 (m), 1360 (w), 1339 (w), 1140−1300 (s), 1118 (m), 1106 (m), 1082 (m), 1021 (s), 969 (s), 952 (m), 928 (m), 905 (w), 874 (w), 862 (w), 842 (w), 809 (w), 763 (w), 744 (m), 730 (w), 667 (w), 635 (s), 623 (m), 610 (w), 575 (m), 515 (s). Elemental analysis for $C_{34}H_{36}Ag_1F_3O_9S$ after crystals were dried in vacuo, found, (calcd) (%): C 52.30, (51.97); H 4.40, (4.62). $^1$H NMR ($CD_3NO_2$, 500 MHz): $\delta$ (ppm.) 3.56 (d, 3H, $^2J_{HH}$ = 13.60 Hz, $CH_2$), 3.82 (s, 9H, OMe), 4.59 (m, 6H, O−$CH_2$), 4.76 (d, 3H, $^2J_{HH}$ = 13.69 Hz, $CH_2$), 5.26 (d, 3H, $^3J_{HH}$ = 11.87 Hz (cis), CH=C$H_2$), 5.38 (d, 3H, $^3J_{HH}$ = 17.10 Hz (trans), CH=C$H_2$), 6.15 (m, 3H, C$H$=$CH_2$), 7.02 (s, 3H, CH aryl), 7.04 (s, 3H, CH aryl).

**X-ray Crystallography.** Crystals were mounted under oil on a glass fiber and X-ray diffraction data collected at 150(1) K with Mo-$K\alpha$ radiation ($\lambda$ = 0.71073 Å) using a Bruker Nonius X-8 diffractometer with ApexII detector and FR591 rotating anode generator. Data sets were corrected for absorption using a multiscan method, and structures were solved by direct methods using SHELXS-97[21] and refined by full-matrix least-squares on $F^2$ by SHELXL-97,[21] interfaced through the program X-Seed.[22] In general, all non-hydrogen atoms were refined anisotropically and hydrogen atoms were included as invariants at geometrically estimated positions, unless specified otherwise. Further details of refinements are given below, and details of data collections and structure refinements are given in Table 1.

Complex **2** did not diffract at high angles, one ligand fragment (type IV in Figure 1) was refined isotropically with a group $U_{iso}$ for the allyl group and C···C distances restrained. Restraints were used on anisotropic displacement parameters of one vinyl group of a different ligand. One $SbF_6^-$ anion was split over two positions and in general the $SbF_6^-$ anions showed signs of dynamic disorder which was not modeled because of a low data/parameter ratio. All F atoms were refined isotropically, and a group $U_{iso}$ was used for the F's of one anion. Residual electron density was modeled as disordered solvent water with O atoms refined isotropically and H atoms excluded. The $SbF_6^-$ anions of complex **3** were highly disordered with the two anions disordered over Sb six positions which were refined anisotropically. The F sites showed considerable disorder, and their refined positions should be regarded as tentative and did not converge. These were given a group isotropic displacement parameter. Restraints were employed on the bond lengths and displacement parameters of one allyl group. In complex **5** the hydrogen atoms on the water ligands and $H_2C$=CH fragments of the allyl groups of the ligands were located in the difference map and refined with restraints on the O−H bond lengths. Some restraints were also used on displacement parameters of the ligands. For complex **7**, the $CF_3$ group of one triflate was severely disordered, and a satisfactory disorder model could not be refined. This group was included at positions where it first appeared in the difference map but not refined.

## Results and Discussion

Ligand **1** was reacted in nitromethane solution with AgX salts in various stoichiometries where X = $BF_4^-$, $ClO_4^-$, $PF_6^-$, $SbF_6^-$, $ReO_4^-$, and $CF_3SO_3^-$. Antisolvent vapor diffusion gave crystalline complexes in all cases, Scheme 1, with the exclusion of $AgPF_6$ and $AgReO_4$ where no crystalline materials were isolated. Different complexes were isolated

(21) Sheldrick, G. M. *SHELXS-97*; *Acta Crystallogr.* **2008**, *A64*, 112.
(22) Barbour, L. J. *J. Supramol. Chem.* **2003**, *1*, 189.

**Table 1.** Details of Data Collections and Structure Refinements

| | **2** | **3** | **4** | **5** | **7** | **8** |
|---|---|---|---|---|---|---|
| formula | $C_{264}H_{315}Ag_9F_{54}O_{61.5}Sb_9$ | $C_{66}H_{72}Ag_2F_{12}O_{12}Sb_2$ | $C_{35}H_{42}AgF_6N_2O_{12}Sb$ | $C_{35}H_{46}Ag_2B_2F_8N_2O_{12}$ | $C_{35}H_{36}Ag_2F_6O_{12}S_2$ | $C_{34}H_{36}AgF_3O_9S$ |
| $M_r$ | 7564.74 | 1744.48 | 994.33 | 1076.10 | 1042.50 | 785.56 |
| crystal size [mm] | 0.4 × 0.4 × 0.4 | 0.4 × 0.1 × 0.07 | 0.3 × 0.3 × 0.07 | 0.22 × 0.05 × 0.01 | 0.1 × 0.03 × 0.01 | 0.24 × 0.03 × 0.02 |
| crystal system | cubic | trigonal | triclinic | monoclinic | monoclinic | monoclinic |
| space group | $Fd\bar{3}c$ | $P3_2$ | $P\bar{1}$ | $P2_1/c$ | $P2_1/n$ | $P2_1/n$ |
| $a$ [Å] | 83.135(2) | 24.4020(8) | 10.1507(9) | 19.863(3) | 19.297(8) | 14.535(4) |
| $b$ [Å] | = $a$ | = $a$ | 12.7184(11) | 23.410(4) | 8.319(3) | 8.3177(18) |
| $c$ [Å] | = $a$ | 13.7461(6) | 16.7933(14) | 9.2250(12) | 27.818(12) | 26.468(7) |
| α [deg] | 90 | 90 | 70.827(4) | 90 | 90 | 90 |
| $\beta$ [deg] | 90 | 90 | 87.684(4) | 98.163(7) | 98.13(2) | 95.451(7) |
| $\gamma$ [deg] | 90 | 120 | 70.810(3) | 90 | 90 | 90 |
| $V$ [Å$^3$] | 574579(24) | 7088.6(5) | 1928.4(3) | 4246(1) | 4420(3) | 3185.4(13) |
| $Z$ | 64 | 3 | 2 | 4 | 4 | 4 |
| $\rho_{calcd}$ [g cm$^{-3}$] | 1.399 | 1.226 | 1.712 | 1.683 | 1.566 | 1.638 |
| $\mu$ [cm$^{-1}$] | 1.230 | 1.040 | 1.295 | 1.018 | 1.059 | 0.773 |
| $\theta$ range [deg] | 1.83, 20.93 | 1.67, 26.31 | 1.29, 36.06 | 2.02, 25.74 | 2.56, 24.07 | 2.57, 26.54 |
| data collected | 102663 | 52484 | 62774 | 30419 | 14812 | 24158 |
| unique data, $R_{int}$ | 12621, 0.0763 | 16829, 0.0575 | 18055, 0.0466 | 8010, 0.0796 | 5270, 0.0439 | 6611, 0.1109 |
| obs. data [$I > 2\sigma(I)$] | 7597 | 8299 | 15078 | 5390 | 3580 | 3782 |
| data/restraints/parameters | 12621/28/1034 | 16829/54/884 | 18055/0/501 | 8010/16/631 | 5270/0/477 | 6611/0/436 |
| $R_1$ [obs. data] | 0.1240 | 0.1113 | 0.0421 | 0.0479 | 0.0680 | 0.0574 |
| $wR_2$ [all data] | 0.3817 | 0.2717 | 0.1259 | 0.1158 | 0.2250 | 0.1334 |
| absolute structure parameter | | 0.06(4) | | | | |
| GOF | 2.437 | 1.421 | 1.034 | 1.015 | 1.038 | 0.986 |

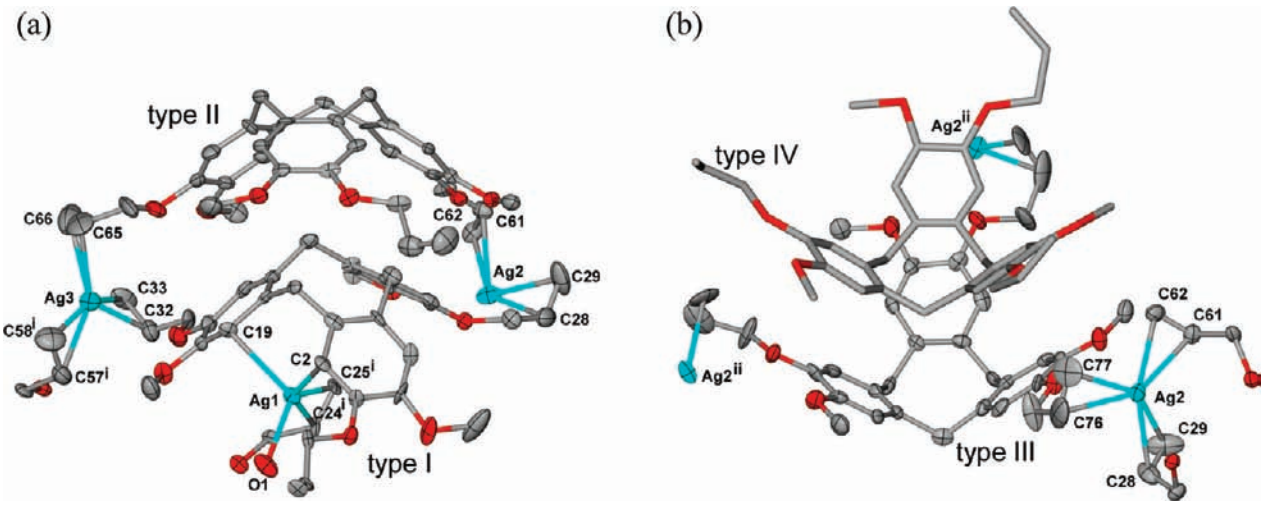


**Figure 1.** From the X-ray structure of $[Ag_9(\mathbf{1})_7(H_2O)_3]\cdot\mathbf{1}\cdot 9(SbF_6)\cdot 10.5(H_2O)$ **2**. (a) Complete coordination spheres of Ag1 and Ag3, with type I (lower) and type II (upper) ligand **1**. (b) Complete coordination sphere of Ag2 along with types III (lower) and IV (upper) ligands. Ellipsoids are shown at 30% probability levels, aside from the isotropically refined "guest" **1** shown in stick representation. Selected bond lengths (Å): Ag1−O17 2.339(15), Ag1−C2 2.571(17), Ag1−C19 2.635(19), Ag1−C24$^i$ 2.420(19), Ag1−C25$^i$ 2.45(2), Ag2−C28 2.58(3), Ag2−C29 2.53(3), Ag2−C61 2.49(2), Ag2−C62 2.46(2), Ag2−C76 2.49(3), Ag2−C77 2.41(3), Ag3−C32 2.53(3), Ag3−C33 2.55(3), Ag3−C65 2.45(3), Ag3−C66 2.45(3), Ag3−C57$^i$ 2.41(2), Ag1−C58$^i$ 2.43(3). Symmetry operations: i: $-z$, 0.5 − $x$, 0.5 − $y$; ii: $y$ − 0.5; 0.75 − $z$, 0.25 − $x$; iii: 0.25 − $z$, 0.5 + $x$, 0.75 − $y$.

through varying anion and reaction conditions. In reactions with $SbF_6^-$ counter-anions, three different complexes were isolated according to reaction stoichiometry and the anti-solvent used. Isolation of the different complexes is repeatable, and each of them features quite different Ag coordination behavior. A metal-to-ligand ratio of 1:3 with diethylether as antisolvent results in the formation of $[Ag_9(\mathbf{1})_7(H_2O)_3]\cdot\mathbf{1}\cdot 9(SbF_6)\cdot 10.5(H_2O)$ **2** whose structure features a 3-D coordination polymer. A 1:1 mixture with diisopropylether as the antisolvent gave a different 3-D coordination polymer within complex $[Ag_2(\mathbf{1})_2]\cdot 2(SbF_6)\cdot n$(solvent) **3**, while a 2:1 metal-to-ligand ratio results in a discrete complex $[Ag_2(\mathbf{1})_2]\cdot 2(SbF_6)\cdot 4(MeNO_2)$ **4**, with the same $Ag_2L_2$ composition as **3**. Interestingly the same reaction conditions that gave complex **3** but with diethylether as the antisolvent give only ligand **1** as the crystalline product.

The identity of the anion also has a marked effect on the nature of the complex isolated. Reactions with the tetrahedral anions $BF_4^-$ and $ClO_4^-$ give iso-structural 1-D coordination chains in $[Ag_2(\mathbf{1})(H_2O)_2]\cdot 2(BF_4)\cdot 2(MeNO_2)$ **5** and $[Ag_2(\mathbf{1})(H_2O)_2]\cdot 2(ClO_4)\cdot 2(MeNO_2)$ **6**. Use of silver(I) triflate gives two different complexes, once again resulting from different metal-to-ligand stoichiometries and different anti-solvents, namely, $[Ag_2(\mathbf{1})(OTf)_2]$ **7** where OTf = triflate from a 3:1 M:L mixture and complex $[Ag(\mathbf{1})(OTf)]$ **8** from a 1:2 mixture, Scheme 1. Unlike the quite disparate structures found for **2** and **3**, the structures of complexes **7** and **8** are broadly similar, both based on 1-D $[Ag_n(\mathbf{1})]^{n+}$ coordination

**Scheme 1.** Different $[Ag_n(\mathbf{1})_m]^{n+}$ Complexes Isolated

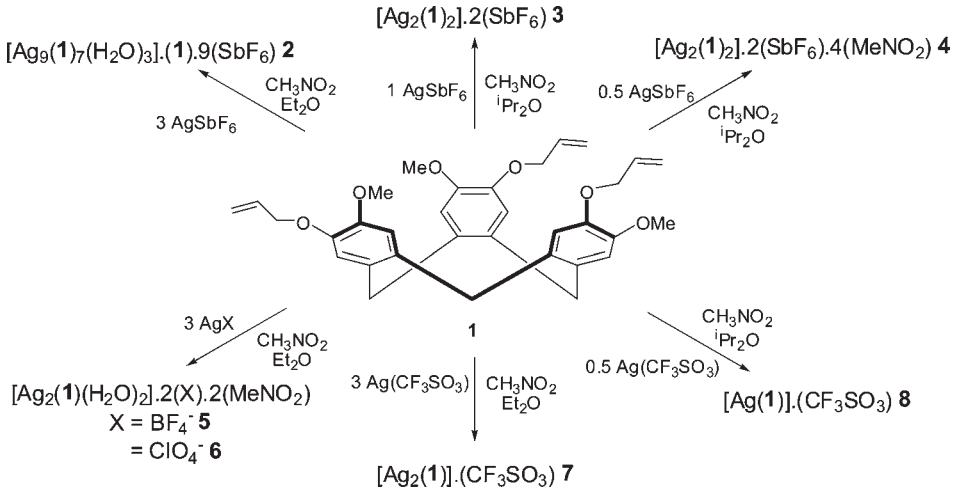


chains linked into either 2-D or 3-D networks by bridging $CF_3SO_3^-$ anions.

**3-D Coordination Polymers and Discrete Capsule with $AgSbF_6$.** The complex $[Ag_9(\mathbf{1})_7(H_2O)_3]\cdot\mathbf{1}\cdot 9(SbF_6)\cdot 10.5(H_2O)$ **2** features a remarkably complicated 3-D coordination polymer. The complex crystallizes in a face centered cubic space group with a very large unit cell volume of $>570{,}000$ Å$^3$. The asymmetric unit comprises two complete ligands and two one-third ligand fragments; three Ag(I) sites; two fully occupied $SbF_6^-$ anions along with one partially occupied $SbF_6^-$ and a fragment of an $SbF_6^-$ sited on a special position; one water ligand, and several ill-resolved solvent positions. All three Ag(I) types have different coordination environments, and these are shown in Figure 1. Ag1 forms $\eta^1$ interactions to two phenyl groups of one ligand **1**, $\eta^2$ interactions to the allyl group of a symmetry-relation of the same ligand **1**, and a terminal water ligand. Organometallic interactions between transition metals and the aromatic rings of CTV or CTV-type ligands have been previously reported, with most examples involving $\eta^6$ interactions to the external face(s) of the host.[23] The bridging $\eta^1$ interactions of Ag1 to the internal host face observed here are very similar to previously reported for an Ag(I) complex of CTV,[19] and similar Ag-host organometallic interactions have been observed with calixarene hosts.[24] Both Ag2 and Ag3 coordinate to three crystallographically distinct host ligands, all through $\eta^2$-allyl interactions, Figure 1.

There are four crystallographically distinct types of ligand **1**, and these occur in pairs throughout the structure. Those designated types I and II are the pair shown in Figure 1a, with type I bound to all three Ag centers while type II only binds to Ag2 and Ag3. This pair of ligands are bound together via Ag centers in a misaligned bowl-in-bowl manner such that a lower rim $-CH_2-$ of ligand type I occupies the guest position of ligand type II. There is one $\pi-\pi$ stacking interaction between the pair at a ring centroid separation of 3.87 Å. The other pair, designated type III and IV ligands, are shown in Figure 1b. These are not linked via Ag centers and show an aligned bowl-in-bowl stacking of a "guest" ligand type IV into the molecular bowl of the type III ligand. The type IV "guest" ligand **1** does not coordinate to any metal centers, hence will be disregarded when discussing the polymeric coordination network. Ligands of type I−III each bind to three metal centers. Ag1 is bound by two ligands, both of type I, while Ag2 and Ag3 are each bound by three ligands, and overall a 3-connected network is formed.

The ligand type I/II pair shown in Figure 1a show further host−guest and coordination interactions between their symmetry equivalent positions. The intracavity guest position of the type I host is occupied by Ag1 and a coordinating allyl group of an adjacent type I ligand. These interactions form a double ring structure of six pairs of Ag-linked type I/II ligand pairs, Figure 2a, with the type I ligands forming the inner ring. The hexa-ring is in an "upright" chair conformation, Figure 2b, enforced by the rigid core of the ligand with arene groups at ~88° to one another and the relatively linear linkages that occur between the ligands. Xu and Warmuth have shown that a molecular cube is formed when eight CTG-fragments are linked in a linear fashion and with all of their molecular bowls converging inward, and a similar cube motif has been reported for the aggregation of hexafunctionalised tribenzotriquinacenes.[16] In the hexa-ring shown in Figure 2, the molecular bowls are convergent and take six of eight cube vertex positions, as shown for the outer ring. Hence the double hexa-ring is essentially a double cube arrangement but with two opposite vertices missing, shown schematically for the outer ring only in Figure 2c. All interactions to the type I inner ring ligands are shown in Figure 2; however, the outer type II ligands are linked to further ligand positions via Ag2 to create the 3-D network, hence subsequent description will disregard Ag1 and the inner ring type I ligand.

For a discrete cube to be formed, additional ligands binding to the hexa-ring fragment would need to do so in a convergent "bowl-in" fashion with one such ligand

(23) (a) Ceccon, A.; Gambaro, A.; Manoli, F.; Venzo, A.; Bitterwolf, T. E.; Ganis, P.; Valle, G. *J. Chem. Soc., Perkin Trans. 2* **1991**, 233. (b) Steed, J. W.; Junk, P. C.; Atwood, J. L.; Barnes, M. J.; Raston, C. L.; Burkhalter *J. Am. Chem. Soc.* **1994**, *116*, 10346. (c) Hancock, K. S. B.; Steed, J. W. *Chem. Commun.* **1998**, 1409. (d) Fairchild, R. M.; Holman, K. T. *J. Am. Chem. Soc.* **2005**, *127*, 16364.

(24) (a) Shelly, K.; Finster, D. C.; Lee, Y. J.; Scheidt, W. R.; Reed, C. A. *J. Am. Chem. Soc.* **1985**, *107*, 5955. (b) Munakata, M.; Wu, L. P.; Kuroda-Sowa, T.; Maekawa, M.; Suenaga, Y.; Sugimoto, K.; Ino, I. *J. Chem. Soc., Dalton Trans.* **1999**, 373. (c) Ikeda, A.; Shinkai, S. *J. Am. Chem. Soc.* **1994**, *116*, 3102. (d) Xu, W.; Puddephat, R. J.; Muir, K. W.; Torabi, A. A. *Organometallics* **1994**, *13*, 3054.

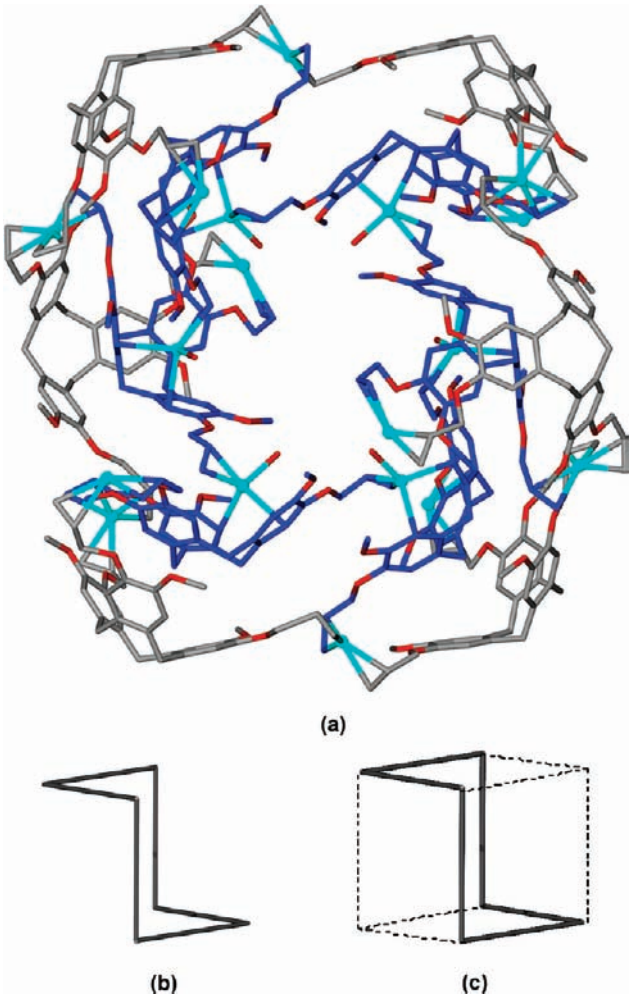


**Figure 2.** (a) Double hexa-ring fragment of the 3-D coordination polymer of $[Ag_9(\mathbf{1})_7(H_2O)_3]^{9+}$ of complex **2** viewed from above. Type I ligands that form the inner ring are shown in blue, while type II ligands that form the outer ring are in gray. (b) Connectivity diagram indicating the ligand positions of the outer hexa-ring viewed from the side and showing the chair conformation. (c) Schematic with dotted lines to the "missing" cube vertices (see text).

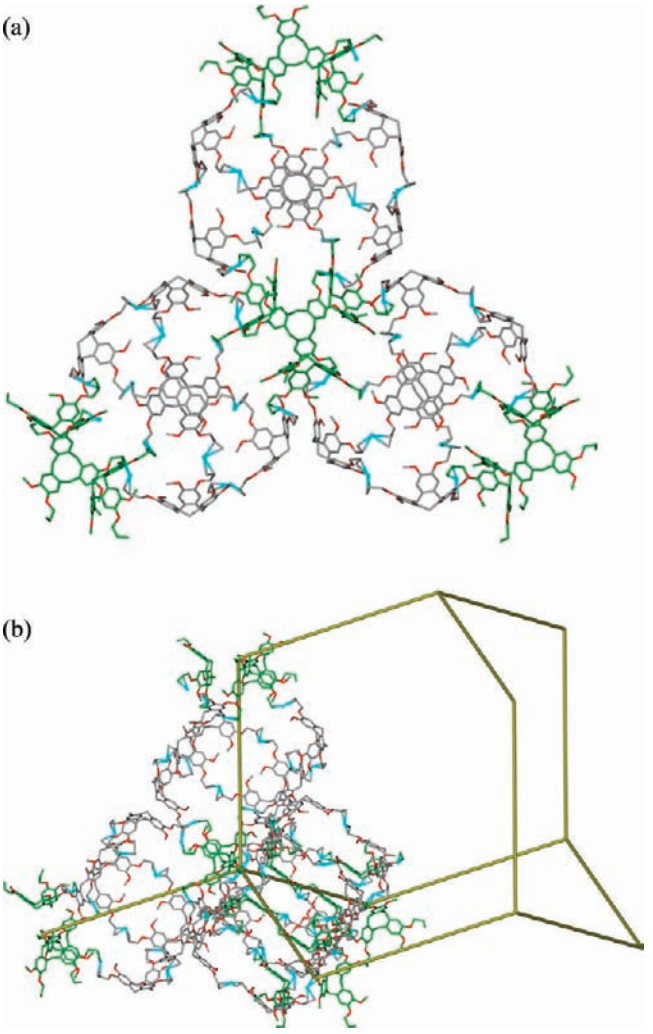


**Figure 3.** Extended network structure of complex **2**. Figures (a) and (b) illustrate how the outer hexa-rings (gray) highlighted in Figure 2 are linked together by ligand type III (green). Ag1 positions, type I and IV ligand **1** molecules, $SbF_6^-$, solvent and hydrogen positions have been excluded for clarity, in (b) the diamondoid relationship between the fragments is indicated by thick lines.

binding to the three Ag2 centers at each of the two "missing" cube vertex sites. Instead, additional ligands bind to Ag2 in a divergent "bowl-out" manner, with each Ag2 center bound by a different symmetry related ligand of type III, Figure 3a. These ligands bridge between hexa-rings to form a 3-D polymer. Each hexa-ring is connected to six type III ligands via Ag2, and these occur in two groupings, with three divergent ligands at each missing cube vertex position. The type III ligands (shown in green in Figure 3) occur in groupings of four such ligands in a tetrahedral arrangement with their molecular bowls facing outward. There are disordered anion and solvent molecules between the ligands within these grouping, and they do not approach each other closely. The simplest way to understand the overall 3-D polymer is by considering the manner in which the convergent type II ligand hexa-rings and the divergent type III ligand groups are linked together. Each grouping of divergent type III ligands bridges between four hexa-rings via Ag2 centers, and each hexa-ring is connected to two groups of the divergent ligands, which occurs in a diamondoid manner, Figure 3b. Overall, the structure is 2-fold interpenetrating with two $[Ag_9(\mathbf{1})_7(H_2O)_3]^{9+}$ networks entangled together, and has no significant channels. Thermal gravimetric analysis (TGA) of **2** showed that it is stable to 200 °C (see the Supporting Information, Figure S1).

The crystal structure of $[Ag_2(\mathbf{1})_2]\cdot 2(SbF_6)\cdot n(\text{solvent})$ **3** also features an unusual 3-D 3-connected coordination polymer. There are two Ag sites, two ligand **1** hosts, and a number of disordered $SbF_6^-$ sites within the asymmetric unit. The two ligands in the asymmetric unit are of opposite chiralities; hence, although this complex crystallizes in a chiral space group, the chirality is not due to a self-sorting of the ligands. Both Ag centers have similar coordination environments, Figure 4, with each being coordinated by one O-allyl moiety through both a coordinate Ag−O interaction and an organometallic $\eta^2$-allyl interaction; and to two other allyl groups in an $\eta^2$ arrangement. Each Ag center is bound by three ligands, hence is a 3-connecting center in the overall network.

Both types of ligands are also 3-connecting centers, each binding to three Ag positions. As for complex **2**, the ligands are arranged in a bowl-in-bowl stacking motif;

however, in complex **3**, the stacking motifs extend in an infinite manner throughout the structure, Figure 5a. Each stack only contains ligands of the same enantiomer. The coordination network is 3-D with large unidirectional channels running along the *z* direction, Figure 5b. The channels are about 19 Å in diameter, and the walls of the channels are helical. All helices within the structure have the same handed screw accounting for the overall chirality of the structure. Highly disordered $SbF_6^-$ anions occupy spaces near the walls of the channels.

Any residual solvent in the channels could not be located in the crystal structure, presumably because of severe disorder. The calculated solvent-accessible void space within the unit cell is about 1370 $Å^3$ [25] which is about 19% of the unit cell volume. Notably complex **3** retains its single crystallinity after evacuation under vacuum. A crystal that had been heated to 50 °C under vacuum for 10 h gave the unit cell parameters: trigonal (hexagonal) $a = 24.4806$, $c = 13.7642$ Å. Attempts to undertake anion-exchange within complex **3** by soaking the crystals in methanol solutions containing NaX where $X = [Co(C_2B_9H_{11})_2]^-$ or $BF_4^-$ anions were not successful, as no anion exchange was indicated by IR studies. TGA showed a gradual mass loss of 28.7% to 250 °C (see the Supporting Information, Figure S2).

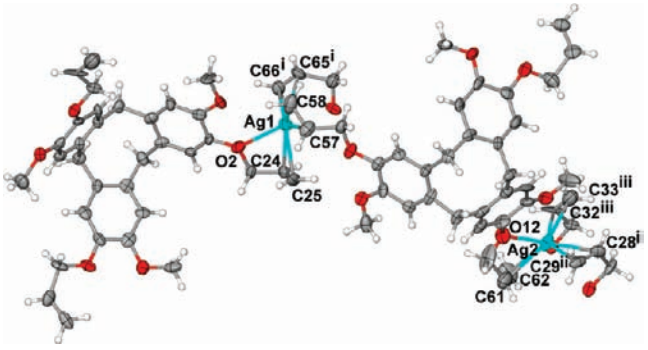


**Figure 4.** Ag coordination environments from the crystal structure of $[Ag_2(\mathbf{1})_2]\cdot 2(SbF_6)\cdot$(solvent) **3**. Ellipsoids are shown at 30% probability levels. Selected bond lengths (Å): Ag1−O2 2.550(10), Ag1−C24 2.581(14), Ag1−C25 2.505(15), Ag1−C57 2.530(15), Ag1−C58 2.35(2), Ag1−C65$^{i}$ 2.599(13), Ag1−C66$^{i}$ 2.442(14), Ag2−O12 2.505(13), Ag2−C61 2.53(2), Ag2−C62 2.51(2), Ag2−C28$^{ii}$ 2.601(17), Ag2−C29$^{ii}$ 2.487(14), Ag2−C32$^{iii}$ 2.469(18), Ag2−C33$^{iii}$ 2.56(2). Symmetry operations: i: $1 - x + y$, $1 - x$, $1/3 + z$; ii: $-y$, $x - y - 1$, $z - 1/3$; iii: $x - 1$, $y$, $z$.

The network connectivities of the 3-D coordination polymers of both complexes **2** and **3** are complicated and highly unusual. Although it is easiest to understand the structure of complex **2** through its diamondoid relationship between fragments, it is actually a 3-connected 3-D network with six different connecting nodes. A simplified connectivity diagram of one of the interpenetrating networks of complex **2** is shown in Figure 6a with connections between ligands of type II and III shown (equivalent to Figure 3). The connectivity diagram of complex **3** is simpler, Figure 6b, with the shortest circuits formed being 8-membered rings and 12-membered rings.

The third complex isolated with $AgSbF_6$ is complex $[Ag_2(\mathbf{1})_2]\cdot 2(SbF_6)\cdot 4(MeNO_2)$ **4** where the Ag complex is a discrete capsule-like dimeric assembly, Figure 7. The capsule is centro-symmetric with one ligand **1** and one Ag(I) in the asymmetric unit along with one $SbF_6^-$ and two $MeNO_2$ solvent molecules. The Ag(I) is coordinated by $H_2C{=}CH$- fragments of two allyl groups, each in an $\eta^2$ fashion (one from the symmetry equivalent ligand **1**) and through $\eta^1$ interactions to two phenyl groups of one ligand, Figure 7. One of the allyl groups of the ligand is not involved in any interactions to a Ag(I) cation. The Ag(I) cations and coordination allyl groups occupy the central space of the capsule. In the crystal lattice the $[Ag_2(\mathbf{1})_2]^{2+}$ capsules pack together into a 2-D grid through $\pi-\pi$ stacking interactions between phenyl groups at ring centroid separations 3.59 and 3.69 Å.

**1-D Coordination Polymers with Tetrahedral Anions.** Slow diffusion of diethylether into a nitromethane solution containing **1** with 3 equiv of either $AgBF_4$ or $AgClO_4$ gave crystals of $[Ag_2(\mathbf{1})(H_2O)_2]\cdot 2(X)\cdot 2(CH_3NO_2)$ where $X = BF_4^-$ (complex **5**) or $ClO_4^-$ (complex **6**). The structures of these complexes with these small tetrahedral anions are isostructural, differing only in the identity of

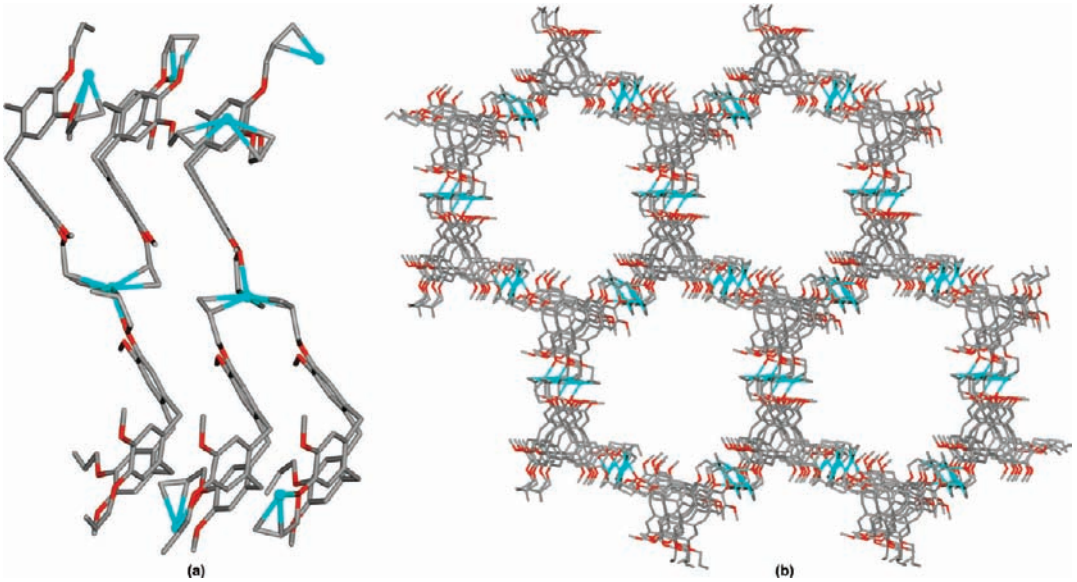


**Figure 5.** 3-D coordination polymer of complex **3** with (a) highlighting the formation of stacks of bowl-in-bowl ligands; (b) showing the helical unidirectional channels viewed down *c*.

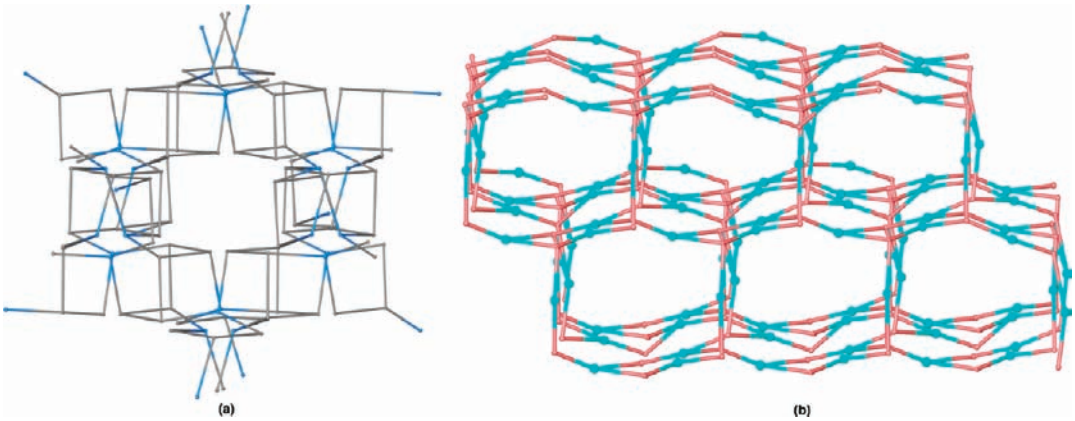


**Figure 6.** Connectivity diagrams for complexes **2** and **3**. (a) One simplified 3-connected network of complex **2** with centers of type II ligand in gray and type III in blue. (b) Network connectivity of complex **3** with Ag centers in blue and ligand centers in pink.

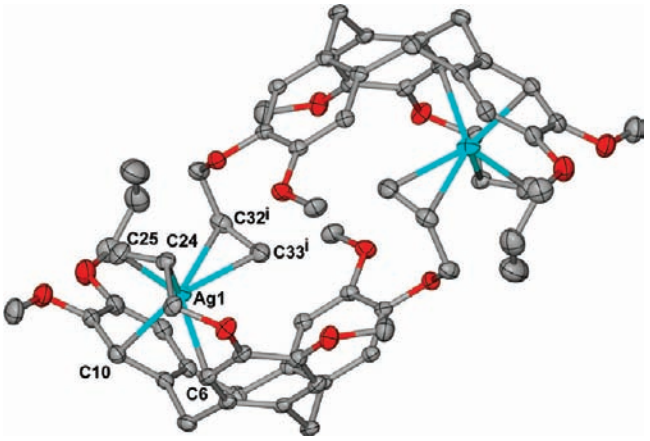


**Figure 7.** Capsule-like structure from the crystal structure of $[Ag_2(\mathbf{1})_2]\cdot 2(SbF_6)\cdot 4(MeNO_2)$ **4**. Ellipsoids are shown at 50% probability levels. Selected bond lengths (Å): Ag1−C6 2.5436(17), Ag1−C10 2.6055(19), Ag1−C24 2.5907(19), Ag1−C25 2.5436(17), Ag1−C32$^{i}$ 2.5094(19), Ag1−C33$^{i}$ 2.430(2), Symmetry operation: i: $2-x, 2-y, -z$.

the anions. Only the structure of the $BF_4^-$ complex, $[Ag_2(\mathbf{1})(H_2O)_2]\cdot 2(BF_4)\cdot 2(CH_3NO_2)$, will be discussed in detail as data from the complex containing $ClO_4^-$ did not refine satisfactorily because of twinning, although is clearly isostructural with **5** and has monoclinic *P* unit cell parameters $a = 19.8435(18)$, $b = 23.2302(21)$, $c = 9.0898(8)$ Å, $\beta = 98.20(1)°$.

There are two Ag(I) positions in the asymmetric unit of $[Ag_2(\mathbf{1})(H_2O)_2]\cdot 2(BF_4)\cdot 2(MeNO_2)$ **5**, and each has a different coordination environment. Ag1 is coordinated by one terminal water ligand, by chelating Ag−O interactions from ligand **1** although one interaction is weak with a Ag···O separation of 2.636(3) Å, and a $H_2C{=}CH$- fragment of the allyl group of an adjacent ligand **1** in a $\eta^2$ fashion, Figure 8. Ag2 is bound by a terminal water ligand, and $\eta^2$ interactions with allyl groups of two symmetry related ligand **1**. Each Ag is bound by two symmetry-related host ligands, and each ligand **1** binds to four Ag(I) positions through the allyl groups of each of the three allyl arms and through the chelating Ag−O coordination interactions. Complex **5** yielded good quality X-ray data

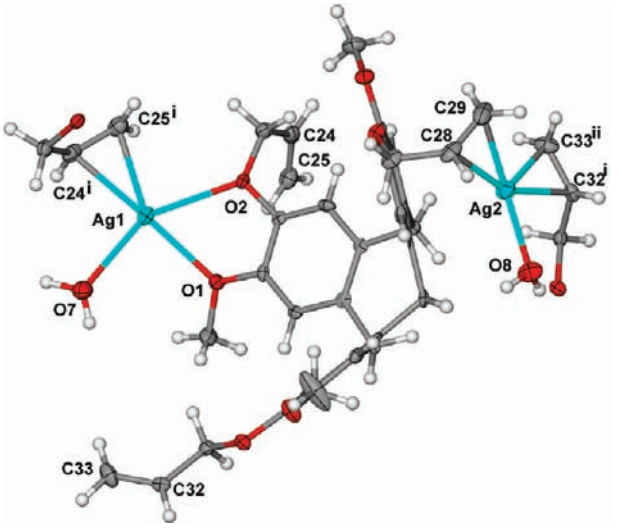


**Figure 8.** From the crystal structure of $[Ag_2(\mathbf{1})(H_2O)_2]\cdot 2(BF_4)\cdot 2(MeNO_2)$ **5**. Coordination environment of Ag(I) cations. Only the O-allyl groups of symmetry-related binding ligands are shown for clarity. Ellipsoids are shown at 50% probability levels. Selected bond lengths (Å): Ag1−O1 2.441(3), Ag1−O2 2.636(3), Ag1−O7 2.477(4), Ag1−C24$^{i}$ 2.442(5), Ag1−C25$^{i}$ 2.430(5), Ag2−O8 2.295(4), Ag2−C28 2.530(5), Ag2−C29 2.413(5), Ag2−C32$^{ii}$ 2.452(5), Ag2−C33$^{ii}$ 2.391(5). Symmetry operations: i: $x, 0.5-y, z-0.5$; ii: $x, 0.5-y, 0.5+z$.

so that all parameters of the allyl groups, including hydrogen atom positions, could be refined. This allows an estimation of the degree of back-bonding present in $\eta^2$-allyl-Ag interactions. The Ag−C distances are all between 2.391(5) and 2.530(5) Å with the interaction to the terminal C always the shortest one which is consistent with the bond lengths reported by Steel et al. for divinylbenzene complexes.[5] The C−C bond lengths of the $H_2C{=}CHR$ groups in **5** are longer than the 1.31−1.32 Å of the native ligand **1**[26] as would be anticipated, at C24−C25 1.368(7), C28−C29 1.349(8) and C32−C33 1.341(7) Å. The longer bond for C24−C25 indicate that this shows the highest degree of back-bonding, and this is supported by the only significant bending away of the C−H groups being observed for this group where the *trans* H−C25···C24−H torsion angle is −164.1°. Weakening of the C=C bonds

(25) SQUEEZE was only used to calculate available space: Spek, A. L. *Acta Crystallogr.* **1990**, *A46*, C34.

(26) Scott, J.; MacFarlane, D. R.; Raston, C. L.; Teoh, C. M. *Green Chem.* **2000**, 123.

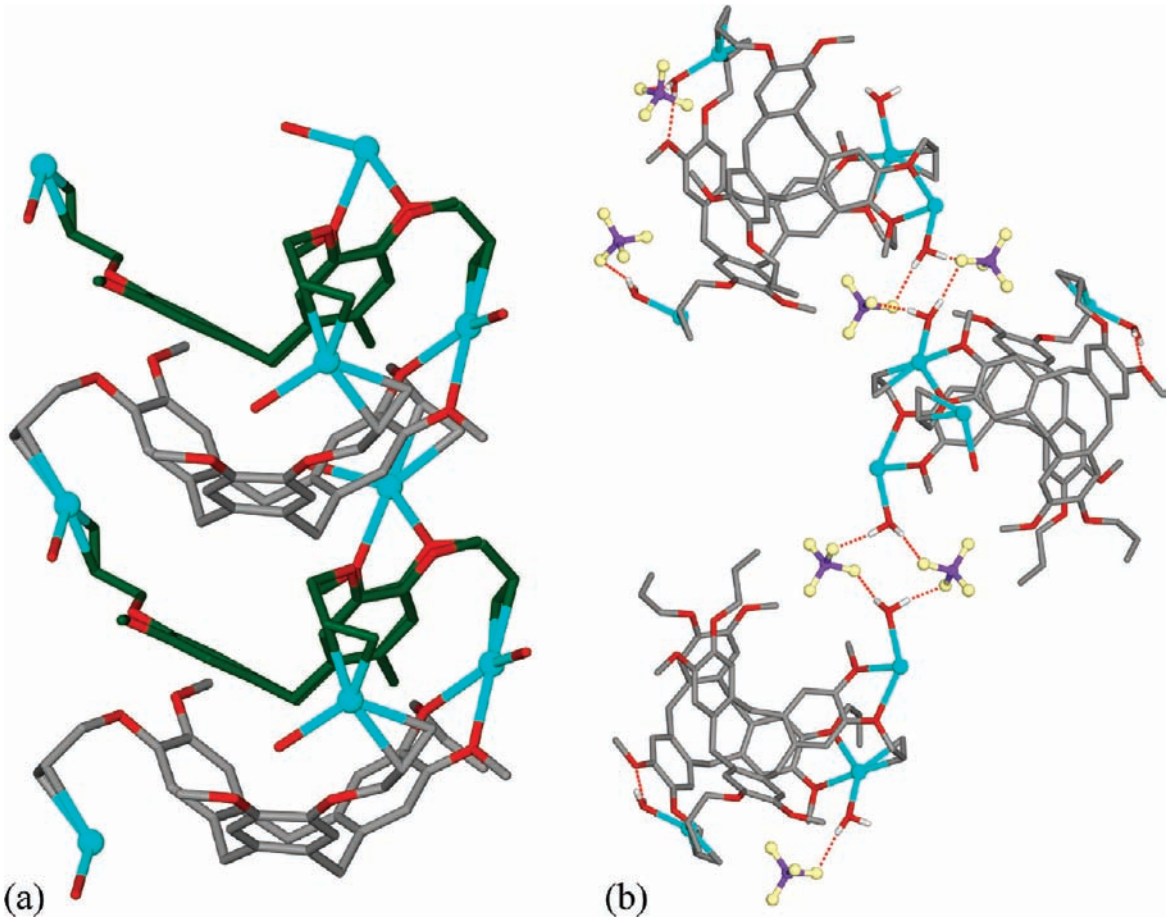


**Figure 9.** (a) Section of a 1-D chain of complex **5** with alternating positions of each enantiomer of the host ligands shown in different colors, and hydrogen atoms excluded; (b) Partial packing diagram of **5** illustrating the hydrogen bonding links between coordination chains via $BF_4^-$ anions (shown in ball-and-stick). For clarity, only hydrogen atoms of the water ligands are shown.

(IR 1607 $cm^{-1}$) was not observed, however, in the IR spectra for any of the crystalline complexes.

Overall each ligand **1** within complex **5** is connected to two others via the Ag(I) centers, with two links to one ligand directly below it and two links to a ligand directly above. A chain structure is thus propagated along the *z* crystallographic direction. Within each 1-D chain the host molecules are positioned in bowl-in-bowl arrangement with one of the lower rim $-CH_2-$ moieties of one ligand position above the center of the molecular bowl of the next ligand, and the third ligand in the series having the same orientation along *z* as the first, Figure 9a. The chain propagates along the glide plane; hence, both enantiomers of the ligand are present within one chain. The structures of CTV and a number of CTV clathrates have essentially the same offset bowl-in-bowl stacking motif.[27] These have very similar relative arrangements of the host molecules and even show similar intermolecular distances of about 4.3−4.4 Å from the guest positioned $-CH_2-$ group of one host to the center of the $-(CH_2)_3-$ lower rim plane of the next.

The orientation of the coordination chains alternates in a checkerboard arrangement throughout the crystal lattice, and there are strong hydrogen bonding interactions between the chains to form 2-D networks overall. Each terminal water ligand forms strong hydrogen bonding interactions as a hydrogen bond donor. These occur between the coordination chains for Ag1-$OH_2$, where interactions with $BF_4^-$ anions result in a bridging $R_4^4(12)$ motif, Figure 9b. Well ordered nitromethane solvent molecules fill the gaps within the lattice.

**Triflate Linked $Ag_2$(1) Coordination Chains.** Use of triflate anions gave complexes whose coordination polymer structures are based on 1-D $[Ag_n(\mathbf{1})]^{n+}$ coordination chains linked into either 2-D or 3-D networks by bridging $CF_3SO_3^-$.

The single crystal X-ray structure of complex $[Ag_2(\mathbf{1})(OTf)_2]$ **7** showed that it has a 3-D coordination network structure. There are two crystallographically independent Ag(I) cations, and these show different coordination behavior. Unlike the 1-D chain structures of $[Ag_2(\mathbf{1})(H_2O)_2]^{2+}$ in complexes **5** and **6**, all silver-ligand interactions are organometallic in nature and include $\eta^2$ interactions with the allyl groups and a phenyl group of the host framework. Ag1 is approximately tetrahedrally coordinated with bonds to two symmetry-related triflate anions, one $\eta^2$-allyl interaction and binds to the external face of the host ligand again through an $\eta^2$ interaction, Figure 10. Ag2 is coordinated through two $\eta^2$-allyl interactions from adjacent ligands and by two symmetry-related triflate

(27) (a) Caira, M. R.; Jacobs, A.; Nassimbeni, L. R. *Supramol. Chem.* **2004**, *16*, 337. (b) Zhang, H.; Atwood, J. L. *J. Crystallogr. Spectrosc. Res.* **1990**, *20*, 465. (c) Birnbaum, G. I.; Klug, D. D.; Ripmeester, J. A.; Tse, J. S. *Can. J. Chem.* **1985**, *63*, 3258. (d) Cerrini, S.; Giglio, E.; Mazza, F.; Pavel, N. V. *Acta Crystallogr., Sect. B* **1979**, *35*, 2605.

anions, Figure 10. One triflate is only weakly bound at an Ag−O distance of 2.647(8) Å, although this is not unusually long for Ag-triflate interactions.[28]

Each allyl group within $[Ag_2(\mathbf{1})(OTf)_2]$ binds to a Ag(I) cation; hence, each ligand **1** binds to four Ag positions overall, and the Ag-ligand **1** interactions lead to the formation of a column of stacked host ligands. The arrangement of the ligands with this stack is quite different to the displaced bowl-in-bowl arrangement seen for $[Ag_2(\mathbf{1})(H_2O)_2]^{2+}$ and $[Ag_2(\mathbf{2})(H_2O)]^{2+}$. Here, a methoxy group of one ligand takes the intra-cavity guest position of an adjacent ligand which in turn, has one of its methoxy groups acting as a guest for a further host in the stack, Figure 11a. The crystal structure of ligand **1** itself shows a remarkably similar stacking pattern of the host molecules.[26] Each silver-ligand stack is homochiral, and stacks of alternating bowl-orientation and chirality are arranged in a checkerboard pattern throughout the crystal lattice and are linked together through bridging triflate anions. Both types of triflate anion bridge between two Ag(I) cations to give the 3-D coordination polymer, Figure 11b. If the $[Ag(OTf)_2Ag]$ bridges are considered as a single connecting unit then the network is 4-connected. There are small channels running in the *y* crystallographic direction that did not contain ordered solvent.

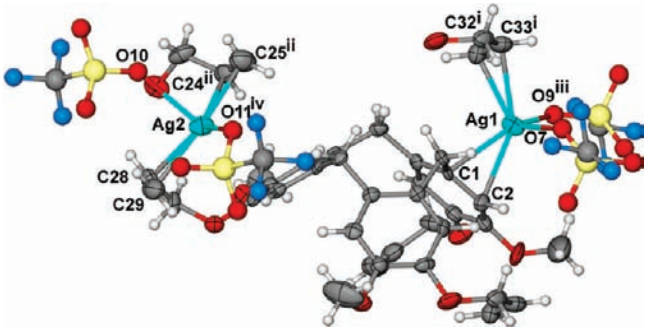


**Figure 10.** X-ray structure of $[Ag_2(\mathbf{1})(OTf)_2]$ **7** showing Ag(I) coordination environment. Ellipsoids are shown at 50% probability levels aside from triflate anions. Selected bond lengths (Å): Ag1−C1 2.571(9), Ag1−C2 2.571(9), Ag1−C32$^{i}$ 2.585(10); Ag1−C33$^{i}$ 2.506(10), Ag1−O7 2.427(10), Ag1−O9$^{iii}$ 2.374(12), Ag2−C28 2.521(12), Ag2−C29 2.429(11), Ag2−C24$^{ii}$ 2.531(1), Ag2−C25$^{ii}$ 2.432(12), Ag2−O10 2.647(8), Ag2−O11$^{iv}$ 2.398(8). Symmetry operations: i: $x$, $1 + y$, $z$; ii: $1.5 - x$, $0.5 + y$, $0.5 - z$; iii: $2 - x$; $-y$, $-z$; iv: $2 - x$; $-y$, $1 - z$.

The structure of complex $[Ag(\mathbf{1})(OTf)]$ **8** shows a similar ligand binding mode to Ag(I) as was seen for Ag2 in complex **7**. The Ag(I) is approximately tetrahedrally coordinated with two $\eta^2$ interactions from allyl groups of symmetry related host ligands, and by two symmetry-related triflate anions, Figure 12a. As for complex **7** only two of the three allyl groups are involved in interactions with the Ag. The Ag-**1** interactions form a 1-D coordination chain very similar to that seen in complex **7**, and these are linked into 2-D networks through bridging triflate anions, Figure 12b. The lack of the second AgOTf unit seen in complex **7** means that the 2-D networks of complex **8** pack together in more space efficient manner, and there are no channels evident in the structure. There are face-to-face $\pi-\pi$ stacking interactions between the networks with a ring centroid separation 3.96 Å.

**Solution Studies.** For each of the complexes, $^1$H NMR spectra were collected of $CD_3NO_2$ solutions containing the same ratios of AgX to **1** that gave the complex. Chemical shift data is given in Table 2 along with that of ligand **1** for comparison. In all cases, coordination induced chemical shifts were observed which were most pronounced for the CH=C$\underline{H}_2$ and C$\underline{H}$=CH$_2$ protons as would be expected for a $\eta^2$-allyl interaction to the Ag. All spectra retained the $C_3$-symmetry of the ligand, which, given the labile nature of Ag−C interactions, is more likely to be due to exchange processes between different species in solution rather than the formation of a single symmetric species. Electrospray mass spectrometry of a 1:2 mixture of $AgSbF_6$ and ligand **1** supports the formation of multiple $Ag_n(\mathbf{1})_m$ species in solution with observed peaks attributable to species $[Ag(\mathbf{1})]^+$, $[Ag(\mathbf{1})_2]^+$, $[Ag(\mathbf{1})_3]^+$, $[Ag_2(\mathbf{1})_3](SbF_6)^+$, and $[Ag_2(\mathbf{1})_2](SbF_6)^+$.

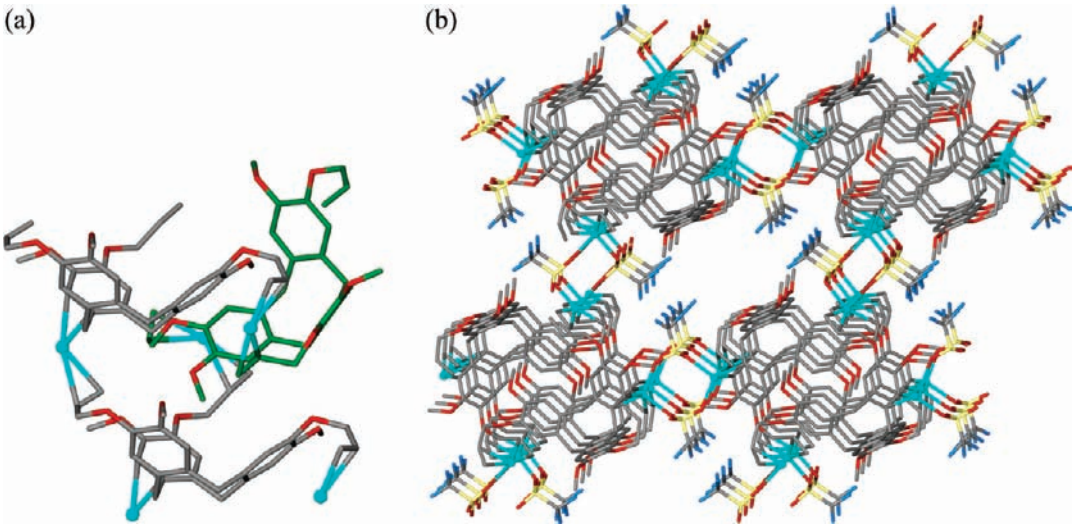


**Figure 11.** X-ray structure of complex **7**. (a) Highlight showing the stacking motif of the ligands with the two different orientations of the ligand within a stack in different colors; (b) packing diagram showing triflate anions bridging between the Ag-ligand stacks to form a 3-D coordination polymer.

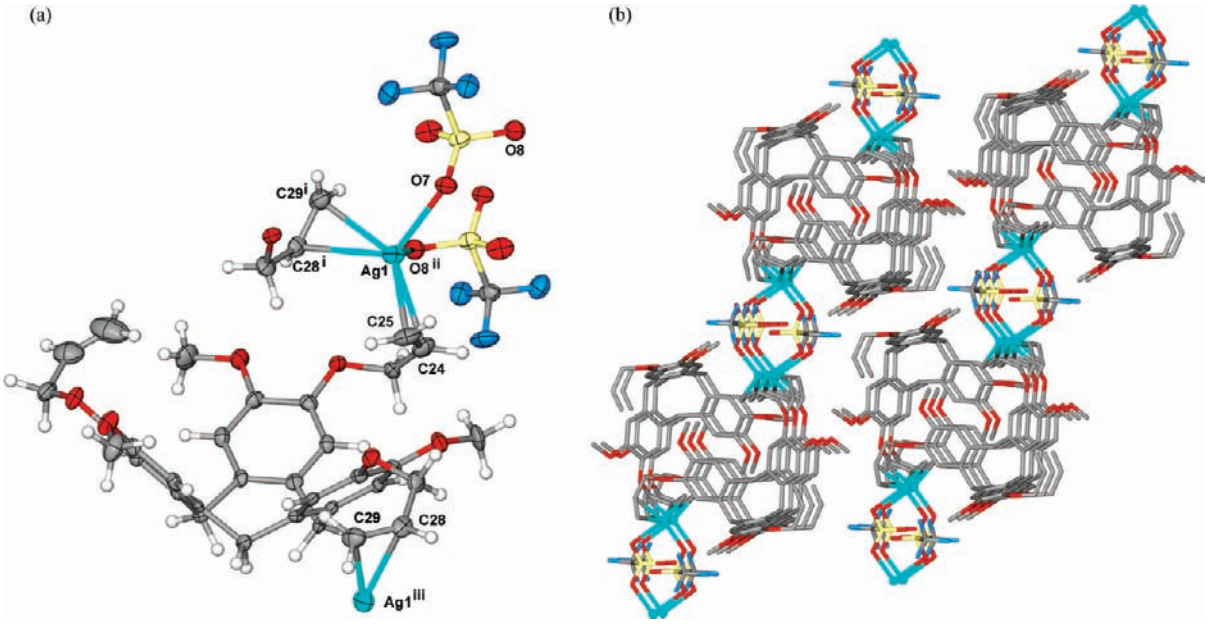


**Figure 12.** X-ray structure of [Ag(**1**)(OTf)] **8**. (a) The Ag(I) coordination environment. Only the O-allyl groups of symmetry-related binding ligands are shown for clarity. Ellipsoids are shown at 50% probability levels. (b) Packing diagram showing triflate bridged 2-D coordination polymers. Selected bond lengths (Å): Ag1−C24 2.487(5), Ag1−C25 2.385(5), Ag1−C28$^{i}$ 2.521(5), Ag1−C29 2.400(5), Ag1−O7 2.363(3), Ag1−O8$^{ii}$ 2.603(5). Symmetry operations: i: 0.5 − *x*, y − 0.5, 0.5 − *z*; ii: 1 − *x*, 2 − y, -*z*; iii: 0.5 − *x*, 0.5 + y, 0.5 − *z*.

**Table 2.** $^{1}$H NMR Shifts (ppm) in $CD_3NO_2$

| compound | $CH_2$ | OMe | O−$CH_2$ | $CH_2$ | cis CH=C$\underline{H}_2$ | trans CH=C$\underline{H}_2$ | C$\underline{H}$=$CH_2$ | CH aryl | CH aryl |
|---|---|---|---|---|---|---|---|---|---|
| ligand **1** | 3.57 d | 3.81 s | 4.57 m | 4.79 d | 5.23 d | 5.35 d | 6.08 m | 7.00 s | 7.02 s |
| **2** | 3.46 d | 3.87 s | 4.53 d | 4.68 dd | 5.43 d | 5.53 d | 6.40 m | 7.06 s | 7.06 s |
| **3** | 3.54 d | 3.84 s | 4.59 m | 4.71 d | 5.30 d | 5.43 d | 6.22 m | 7.03 s | 7.03 s |
| **4** | 3.55 d | 3.83 s | 4.59 m | 4.73 d | 5.39 d | 5.42 d | 6.19 m | 7.03 s | 7.05 s |
| **5** | 3.59 d | 3.83 s | 4.60 m | 4.79 d | 5.28 d | 5.40 d | 6.16 m | 7.03 s | 7.05 s |
| **6** | 3.49 d | 3.90 s | 4.56 d | 4.73 dd | 5.52 d | 5.61 d | 6.54 m | 7.09 s | 7.09 s |
| **7** | 3.53 d | 3.88 s | 4.5−4.75 | 4.5−4.75 | 5.48 d | 5.59 d | 6.49 m | 7.09 s | 7.10 s |
| **8** | 3.56 d | 3.82 s | 4.59 m | 4.76 d | 5.26 d | 5.38 d | 6.15 m | 7.02 s | 7.04 s |

## Conclusions

The tris-allyl CTV-analogue **1** can bind to Ag(I) through organometallic $\eta^2$-allyl and aryl interactions and coordination interactions through the OR groups, and all of these modes are observed in the different complexes reported here. The dominant coordination mode is the $\eta^2$-allyl organometallic interaction, and this is supported by NMR studies in solution. In general, the combination of Ag(I) with ligand **1** produces coordination polymers, and a strong anion influence is observed on the resultant structures. Different complexes were also isolated from different stoichiometric mixtures in the cases of $AgSbF_6$ and $Ag(CF_3SO_3)$. The 3-D coordination polymer of complex $[Ag_9(\mathbf{1})_7(H_2O)_3]\cdot\mathbf{1}\cdot 9(SbF_6)\cdot 10.5(H_2O)$ **2** shows a remarkably complicated, and to the best of our knowledge, unique structure that nevertheless can be related to a simpler 2-fold interpenetrating diamondoid motif. The 3-D coordination polymer of complex $[Ag_2(\mathbf{1})_2]\cdot 2(SbF_6)$ **3** has large unidirectional channels within a robust structure.

**Acknowledgment.** We thank the EPSRC for their financial support of this research, and Ian Blakeley for performing elemental analyses

**Supporting Information Available:** X-ray crystallographic data for complexes **2**−**5**, **7**, and **8** in CIF format. TGA for complexes **2** and **3** (Figures S1 and S2). This information is available free of charge via the Internet at http://pubs.acs.org.

(28) For examples of Ag-$O_3SCF_3$ interactions 2.6−2.7 Å with coordination polymers see ref 3h and also: (a) Rim, C.; Zhang, H.; Son, D. Y. *Inorg. Chem.* **2008**, *47*, 11993. (b) Chen, X.-D.; Mak, T. C. W. *Chem. Commun.* **2005**, 3529. (c) Carlucci, L.; Ciani, G.; Proserpio, D. M.; Rizzato, S. *CrystEngComm* **2002**, *4*, 413.